24th COBEM - 2017

24th ABCM International Congress of Mechanical Engineering
December 3-8, 2017, Curitiba, PR, Brazil

COBEM-2017-0304
USE OF ARTIFICIAL NEURAL NETWORKS FOR IDENTIFICATION OF THE ELECTRIC SUBMERSIBLE PUMP PERFORMANCE WORKING WITH A VISCOUS FLUID

Luis Felipe Barrera Salamanca
Alberto Luiz Serpa
Natache Arrifano Sassim
Jorge Luiz Biazussi
William Monte Verde
University of Campinas (UNICAMP) - Campinas - Brazil
luis.salamanca@fem.unicamp.br
serpa@fem.unicamp.br
natache@cepetro.unicamp.br
biazussi@unicamp.br
williammonteverde@gmail.com

Abstract. *The methods of artificial lifting are fundamental in the petroleum industry for initiating or incrementing the production of wells that have insufficient reservoir energy to raise the fluids to the surface. In this case, the use of Electric Submersible Pump (ESP) is very important. For the petroleum industry, it is important to determine the ESP's performance working with viscous fluids. Therefore, in this paper, an Artificial Neural Network is proposed to identify the behavior of pump working with glycerin. Two different ANN structures were tested to identify the ESP's performance, the Multilayer Perceptron and the Neural Network Finite Impulse Response, and the best structure was chosen through various validation tests. This paper also proposes to compare the response of the best ANN structure with a correlation proposed by Biazussi (Biazussi, 2014) on ESP working with viscous fluid and low viscosity in single-phase flow.*

Keywords: *Artificial Neural Network, Multilayer Perceptron, Neural Network Finite Impulse Response, Electric Submersible Pump, Dimensionless coefficients.*

1. INTRODUCTION

The ESP is a hydraulic machine that transforms the mechanical energy from the electric motor into kinetic energy of the liquid it transports. The kinetic energy is transformed into pressure energy through the stator. The ESP's performance is tested by running it at a constant speed while varying the pumping rate by throttling the flow at the pump discharge. During testing, the flow rate, the brake horsepower and the suction and discharge pressures are measured to determine pump performance. Based on measurements at different flow rates, there are three different parameters to the pump performance: *Head developed* by the pump, *pump's power efficiency* and *brake horsepower*. These are the parameters used to determine the curve of the pump, as show in Figure 1. Usually, these characteristic curves are provided by the manufacturer for operation with water (Takács, 2009).

There are different analysis to determine the characteristic parameters on ESP pumps, one of which is the dimensionless analysis. These dimensionless parameters are used for the design and testing of pumps, as they enable scaled transport of performance characteristics between different operating conditions. These parameters come from the *pi theorem of Buckingham*. There are two evaluation parameters for a pump: *Head* (H) expressed in energy by mass units and *shaft power* $(\dot{W})$. These parameters are function of flow rate (q), angular velocity of rotor (ω), rotor diameter (D), roughness (ϵ), viscosity (μ) and specific mass (ρ) (Monte Verde, 2016). From the application of the concepts of the dimension analysis previously described, four dimensionless groups in each relation are obtained, defined as:

- Head Coefficient

$$\Psi = \frac{\Delta P}{\omega^2 \rho D^2} \tag{1}$$

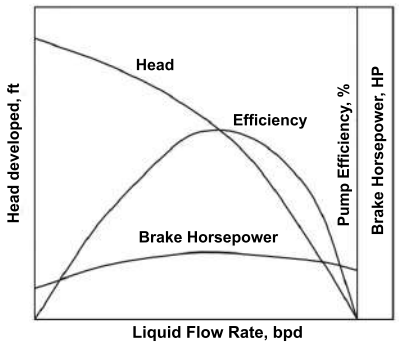

Figure 1. Schematic pump performance curves (Takács, 2009).

- Flow Coefficient

$$\phi = \frac{q}{\omega D^3} \tag{2}$$

- Power Coefficient

$$\Pi = \frac{P_m}{\rho \omega^3 D^5} \tag{3}$$

- Inverse of the rotational Reynolds number

$$X = \frac{1}{Re_w} \tag{4}$$

where the rotational Reynolds number are defined by:

$$Re_w = \frac{\rho \omega D^2}{\mu} \tag{5}$$

For the petroleum industry, it is very important to determine the ESP's performance and the range of operation. For that reason, researchers have based their studies on these dimensionless numbers to propose correlations or mathematical models to describe the behavior and operational conditions of ESP working with viscous fluids or low viscosity fluids.

The ESP working with viscous fluids presents an impact on the operational conditions, reducing the energy transferred and the efficiency of the pumping process if the viscosity increases. The optimum operational range of ESP operating with viscosity fluids is smaller than operating with water (Sirilo, 2013).

There are empirical procedures for correcting performance of conventional centrifugal pumps, such as the *Hydraulic Institute Abacus - USA* (Hydraulic Institute, 2010), obtained from statistical analysis in the 1950s, which are also used to correct the ESP's performance. A process like the one of the Hydraulic Institute Abacus does not contemplate the operation factors complexity involved in ESP, given the constructive and operational specificities. Therefore, it is necessary to propose new methods of corrections of the operational variables under the effect of viscosity variation, whether empirical, strongly supported by experimentation with fluids of higher viscosities than water, or searching models to support a greater understanding of the physical phenomena that occurs in an energy transfer process. Some authors that have worked in this area are briefly listed below.

Solano (Solano, 2009) proposed a mathematical model that allows the mapping of the performance of a pump stage, performing a dimensional analysis to identify which dimensionless groups are important. The functional relationship between these dimensionless groups must be obtained experimentally, being very complex to obtain a solution applicable to any model.

Paternost (Paternost, 2013) worked in a mathematical model to establish a data interpretation method for the characterization of ESP operating with fluid (single phase or biphasic flow). The simplifying hypothesis of this problem was: one-dimensional flow, permanent flow, uniform flow along the rotor, constant rotational speed and disregarding torque by surface and field forces.

Biazussi (Biazussi, 2014) developed a mathematical model that aims to represent the pressure gain and pump shaft power. The dimensionless idealized approach requires single-phase experimental data to adjust the geometric constants

and experimental two-phase data for the adjustment of the slip model constants. The approach adopted here is to propose correlation models, based on fundamental physical phenomena that can be adjusted to the data and enable later interpretation. The equation developed by Biazussi (Biazussi, 2014) is:

$$\Psi = \frac{1}{4} - k_4 + (-k_1 - Xk_2 + 2k_4k_5)\,\phi + \left[-\left(\frac{X}{\phi}\right)^n k_3 - k_4{k_5}^2 - k_6\right]\phi^2 \tag{6}$$

where the k_n variables are pump pressure curve adjustment constants, and just one of these variables depends only on the pump geometry, k_1.

Monte Verde (Monte Verde, 2016) developed an experimental assembly in order to allow evaluation of a conventional ESP performance operating with viscous flow, both single phase as two phase. This experimental apparatus was used to investigate the effects of rotation, suction pressure, liquid flow rate, viscosity and installations inclination on pump operation. The experimental results of pump performance operating with single-phase viscous flow were compared to the main correction methods available in the literature and a specific correction method for the ESP model tested was proposed.

Therefore, based on previous works and fundamental theory of dimensionless coefficients in ESP, this paper proposes the use of an Artificial Neural Network (ANN) structure (based on optimum neurons numbers and optimal hidden layers) that better approximates the ESP's performance based on the dimensionless coefficients.

This paper is organized in 5 sections. In Section 1, an introduction of the ESP working with viscous fluid is presented. Section 2 presents general notions about Artificial Neural Network. Section 3 presents the system identification with the ANN, the procedure of data acquisition, model structure selection phase, model estimation phase and the model validate phase. Section 4 shows the results of the best, among the two alternatives of tested neural network structure, and a comparison with Biazussi's mathematical model. Finally, Section 5 presents the main conclusions.

2. ARTIFICIAL NEURAL NETWORK

Artificial neural networks (ANN) are nonlinear approximators that can be described as mapping an input space to an output space (Priddy and Keller, 1985). They are composed of many simple elements operating in parallel called "neurons", which are the fundamental units of an ANN. These elements are inspired by the biological nervous systems (Cruz, 2010). The function of the neural network is predominantly determined by the connections between the elements called synaptic weights (Nørgaard *et al.*, 2001). An ANN can be trained to perform a specific function by adjusting the synaptic weights associated with the connections between the elements. The scheme of a neuron is described in Figure 2 where the output y_k is given by:

$$y_k = \varphi\left(\sum_{j=1}^{m} w_{kj}x_j + b_k\right) \tag{7}$$

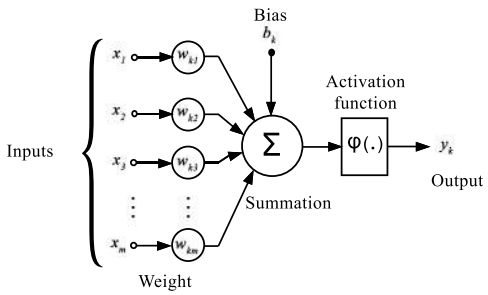

Figure 2. A neuron model (Haykin, 2008).

The functioning of a neuron consists of multiplying the values of the inputs x_j by the synaptic weights W_{kj}. There is and additional pseudo-input for the neuron called bias b_k, which allows the activation function φ to assume a value even when all inputs x_j are zero (Haykin, 2008). The index k refers to the number of the current neuron that is being processed. The most commonly used activation functions are: the linear function, the hyperbolic tangent function, the sigmoid function and the step function. The process of connection between neurons leads to the generation of synapses and the construction of the ANN.

2.1 Learning phase

It is called learning, training or estimation, the process of configuring an ANN so that the inputs generate the desired outputs by strengthening the connections (Cruz, 2010). One way to do this is to determine the optimal values of the synaptic weights matrix W of all neuron connections (Nørgaard *et al.*, 2001). The learning process can be divided in two forms: supervised or unsupervised. For the first case, used in this project, a set of input and output data of the system, obtained through an experiment or simulation, is needed, and the second one focuses on finding statistical characteristics among groupings of patterns in the inputs (Cruz, 2010).

Through an iterative process, the values of the synaptic and bias weights are obtained in such a way that the network, according to a function of performance or cost function, models the relation between the input and output vectors of a given system (Zambrano, 2013). This process is represented schematically in Figure 3, where u is the input signal applied to the plant to be identified by ANN, y is the output of the plant and $\hat{y}$ is the estimated output by ANN.

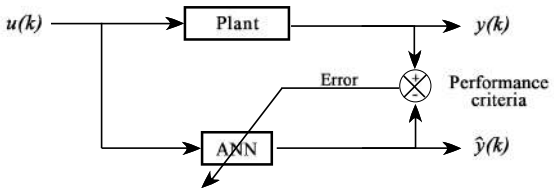

Figure 3. Scheme of an ANN learning process (Zambrano, 2013).

In this process, the outputs are compared with a performance criterion in order to adjust the synaptic weights W by means of an optimization process.

2.2 Optimization process

The objective of the learning process is seen as an optimization problem, whose purpose is to search for the minimum value of the performance criterion. The most commonly used measure of performance is the mean squared error (MSE) (Haykin, 2008), which is calculated by:

$$E(W) = \frac{1}{2N}\sum_{i=1}^{N}[y_i - \hat{y}_i(u, W)]^2 = \frac{1}{2N}\sum_{i=1}^{N} e^2(u, W) \tag{8}$$

where N is the vector data length and W is a weights matrix.

The values of the synaptic weights W that best fit the mapping of the input set u to the output set y are obtained by solving the optimization problem presented in Equation 9 (Nørgaard *et al.*, 2001), where W^* represents the optimal values of the synaptic weights.

$$W^* = \min_{W} E(W) \tag{9}$$

There are many optimization methods and the respective choice depends on the main features of the considered problem. In ANN, the most common method of first-order optimization is the *backpropagation* algorithm, which is a specific implementation of the gradient method (Haykin, 2008). Among the most used second-order optimization methods are: Newton's method, Quase-Newton, Gauss-Newton and Levenberg-Marquardt method (Nørgaard *et al.*, 2001). These methods are characterized by using a Hessian matrix (second derivative).

2.3 Generalization and cross-validation

One of the major advantages of the ANN is their ability to generalize. This means that a trained ANN could classify data from the same class as the training data that has never seen before. To reach the best generalization, the data set should be divided into three parts: training, validation and testing.

The training set is used to train an ANN. The testing set is used to determine the performance of a neural network on patterns that are not trained during training, and the validation set is used for finally checking the overall performance of an ANN.

A cross-validation is a standard tool in statistics that uses the division of the data set previously described to validate the model with a data set different from the one used for parameter estimation. The goal of cross-validation is to define a data set to test the model in the training process, in order to limit problems like overfitting, given an insight on how the model will generalize with an independent data set. With the cross-validation, the training process should be stopped in

the minimum of the test set error. At this point, the ANN generalizes in the best form. When learning is not stopped, overfitting occurs and the performance of the ANN on the whole data decreases, despite the fact that the error on the training data still gets smaller (Haykin, 2008).

3. SYSTEM IDENTIFICATION WITH NEURAL NETWORK

System identification is the task of inferring a mathematical description of a dynamic system from a series of measurements on the system. This technique is used in prediction, fault detection and control system design (Nørgaard *et al.*, 2001). In this case, if the system identification is based exclusively on measured data, assuming only a small knowledge about the physics of the system, the identification process is called *"black box modeling"* (Haykin, 2005).

When attempting to identify a model of a dynamic system, it is a common practice to follow the procedure depicted in the following:

- **Experiment phase**. The purpose of the experiment is to collect a data set that describes how the system behaves over its entire range of operations. The idea is to vary the inputs and observe the impact on the outputs.
- **Model structure selection phase**. A model structure is a set of candidate models based on two things. The first one, select a "family" of model structure considered appropriate for describing the system, e.g., linear model, multilayer perceptron network, etc. The second one, select a subset of the chosen family of model structures. In the family of nonlinear structure, this can for instance be an NNFIR(3,2,1) model structure, where (3,2,1) signifies a time delay of one sampling period.
- **Model estimation phase**. Once a set of candidate models has been chosen, the next step is to pick one particular model from this set. The most common strategy is to pick the model that provides the best one-step ahead predictions in terms of the smallest expected squared error between observed outputs and predictions.
- **Model validation phase**. When a model has been estimated, it must be evaluated to investigate whether or not it meets the necessary requirements. The validation is closely connected to the intended use of the model.

Each step of the procedure used for modeling the ESP performance operating with viscous single-phase flow is presented in the following.

3.1 Experiment phase

Aiming to identify the EPS's performance operating with a viscous liquid flow, an experimental test loop was assembled. The experimental facilities were assembled at LABPETRO, a laboratory from Center of Petroleum Studies (CEPETRO) from University of Campinas (UNICAMP).

This circuit consists of a conventional ESP HC20000L with three stages Baker Hughes ® driven by a three-phase induction motor $380\ V$, $50\ hp$, controlled by a variable speed drive. The system allows for ESP testing with water or glycerin. The test circuit can operate with a maximum flow rate of $65\ m^3/h$ of water or $100\ m^3/h$ of glycerin and a pressure of up to $1\ MPa$ in the suction of the ESP and $2\ MPa$ in the discharge line. A schematic layout of the circuit is shown in Figure 4.

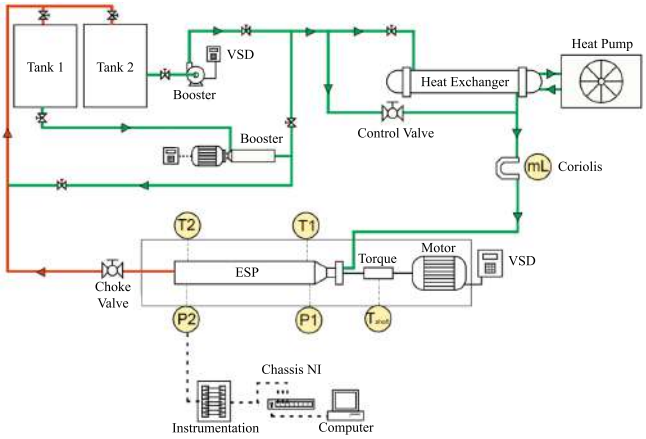

Figure 4. ESP bench test, located at the University of Campinas.

A data set that describes the performance of an HC20000L ESP working with a viscous fluid (glycerin) is used. The operational range data for this pump is presented in Table 1.

Table 1. Measured data to HC20000L Baker Hughes ® ESP.

Rotational Speed [RPM]	Viscosity [cP]	Curves	Total samples
1200	79, 205, 375, 445, 708, 740, 1046, 1566	8	950
1800	80, 195, 436, 752, 1069, 1407	6	
2400	66, 203, 427, 753, 1062, 1387	6	
3000	67, 198, 422, 443, 728, 943, 1362	7	
3500	67, 195	2	

This analysis allows the verification and study the performance of the pump working with the viscous fluid, varying the temperature and the viscosity of the fluid for 5 different rotational speeds. In these measurements, it was verified how the viscosity affects the pump performance, decreasing the pump's *Head*, pump's *efficiency* and increasing the pump's *brake horsepower*. Each point was taken at a sampling rate of 4000 Hz for 30 seconds for a total of 120000 samples. The mean of those samples was calculated to obtain a point on the curve. Therefore, 950 samples to obtain 29 *Head - flow rate* curves were taken.

3.2 Model structure selection phase

Based on a measured data set, two different structures of ANN were tested to describe the pump's performance with viscous fluid. These structures were the multilayer perceptron (MLP) and the Neural Network Finite Impulse Response (NNFIR). These structures were chosen to verify the behavior of the network with delays and without delays in inputs data.

According to (Stepanoff, 1957), the pump performance can be determined using the dimensionless variables previously shown. Thus, the dimensionless variables X, Ψ and ϕ were calculated using the obtained data. With these calculated variables, the inputs and output of the ANN were defined as shown in Table 2.

Table 2. Data set used for system identification based on dimensionless variables.

	Variable	Max	Min	Samples	Curves
Inputs	X	5.543e-4	1.517e-4	950	29
	ϕ	5.746e-2	2.510e-7		
Output	Ψ	1.233e-1	4.580E-3		

With the inputs defined, the two previously mentioned structures, MLP and NNFIR are explained below.

3.2.1 The Multilayer Perceptron

One of the most common ANN structure is the multilayer perceptron (MLP) network. The MLP is an artificial neural network composed of many perceptrons. The basic MLP network is constructed by ordering the neurons in layers, where the output of each neuron from a preceding layer is the input to all neurons in the next layer. The layers that lie between the exit and the entry layers are known as hidden layers (Hornik, 1989). Due to the structure, this type of network is often referred to a *feedforward network*. The MLP utilizes a supervised learning technique called *backpropagation* for training. This MLP is good for learning nonlinear relationships from a set of data (Nørgaard *et al.*, 2001). These structures are shown in Figure 5(a).

The computations performed by such a *feedforward network* with a single hidden layer with nonlinear activation functions and a linear output layer can be written mathematically as:

$$\hat{y} = B\varphi(Ax + a) + b \tag{10}$$

where x is a vector of inputs and $\hat{y}$ a vector of outputs. A is the matrix of weight of the first layer, a is the bias vector of the first layer. B and b are, respectively, the weight matrix and the bias vector of the second layer. The function φ denotes an elementwise nonlinearity.

3.2.2 Neural Network Finite Inpulse Response

The NNFIR is a nonlinear model where the predictors (outputs) are always stable because there is a pure algebraic relationship between predictions and past measurements and inputs. The predictors are given by

$$\hat{y}(t, \theta) = g\left[(\varphi(t, \theta)), \theta\right] \tag{11}$$

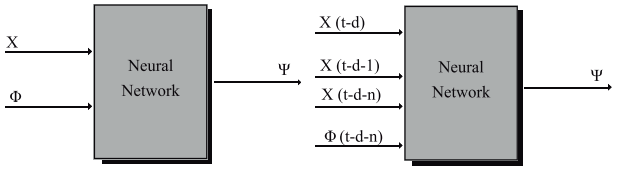

Figure 5. Structures of ANN (a) MLP Network (b) NNFIR Network.

and the input vector is given by

$$\varphi(t) = [u(t-d), ..., u(t-d-n)]^T \tag{12}$$

where θ denotes the adjustable parameters vector (the weights and biases), u is the control inputs, d is the delay, n is the number of delays and g is the function realized by the neural network.

These structures are shown in Figure 5(b).

3.3 Model estimation phase

An algorithm in Matlab was applied to verify the techniques discussed in this work. The Levenberg-Marquardt algorithm was used for the optimization problem solution. This method is very efficient when the ANN is formed by several synapses weights. Although computational requirements are much larger for each iteration, this is offset by the increased efficiency of the method. More information about the Levenberg-Marquardt algorithm can be found in (Hagan and Menhaj, 1994).

For a good comparison, one to twenty neurons for each structure were chosen and one to two hidden layers for each structure were chosen as well. The number of delays is known as the *Lag Space* (n) and this parameter can be empirically determined (Nørgaard *et al.*, 2001). The activation function for hidden layers was a sigmoid function and for the output layer was a linear function. The NNFIR structure was tested in this work for $n = 2$ and $n = 3$. All the results were based on the minimum MSE and the coefficient of determination (R^2).

For the model estimate, a data set measured in the experiment was divided into three different groups, as shown in Table 3. The training set and test set were used for the training process and the validation set was used for the validation process.

Table 3. Division data for model estimation phase and model validation phase.

Data set	Sample porcentage [%]	Samples number
Training	65	618
Test	10	95
Validation	25	237

Each structure was trained with a cross-validation algorithm. For each training, the MSE and the coefficient of determination (R^2) were calculated and the ANN trained was stored. Finally, the MSE and the coefficient of determination were stored in a matrix.

More information about the network training process can be found in Norgaard (Nørgaard *et al.*, 2001) and (Haykin, 2008).

3.4 Model validation phase

After the model estimation phase, the validation set to validate all the ANN was used. The validation data set was not used for the model estimation phases, then, the use of this data set for validating the model is a great parameter to compare the ANN performance with samples that the ANN had never seen. An algorithm to find the minimum value of the error and the maximum coefficient of determination in the matrix that was created in the model estimation phase was made. The result of this algorithm is the best structure of the ANN giving an idea about its generalization.

4. RESULTS AND DISCUSSION

Table 4 shows the evaluation parameters for an MLP and NNFIR structure for training and validation process. It is observed that the MSE error and the coefficient of determination for the validation process are lower than for the training process.

The parameters for analysis were the hidden layer's number, the neuron's number, the coefficient of determination R^2 and the MSE error for both phases. For the MLP structure, the optimum performance was 2 hidden layers with 10 neurons

Table 4. Training and validation results for the MLP and NNFIR structures.

Structure	**Hidden layers**	**Lag space**	**Neurons**	**Training**		**Validation**	
				R^2	*MSE*	R^2	*MSE*
MLP	1	-	13	0.9984	1.6009e-6	0.9977	1.8806e-6
MLP	2	-	[10 8]	0.9991	7.4575e-7	0.9983	1.3773e-6
NNFIR	1	2	5	0.9979	2.4955e-6	0.9972	2.1554e-6
NNFIR	1	3	5	0.9968	2.5344e-6	0.9974	2.0261e-6
NNFIR	2	2	[4 9]	0.9984	1.2790e-6	0.9979	1.6165e-6
NNFIR	2	3	[3 14]	0.9989	8.7608e-7	0.9981	1.5283e-6

in the first hidden layer and 8 neurons in the last hidden layer based on the MSE error and the coefficient of determination. The MLP with 1 hidden layer has a smaller coefficient of determination and smaller MSE error than the MLP structure with 2 hidden layers for the training and the validation phase, then, the MLP with 1 hidden layer was discarded. Figure 6 shows the linear regression of the MLP for the validation data set and a histogram of the absolute error distribution. The purpose of this histogram is to roughly assess the probability distribution of a given variable by depicting the frequencies of observations in bars that occur in certain ranges of values.

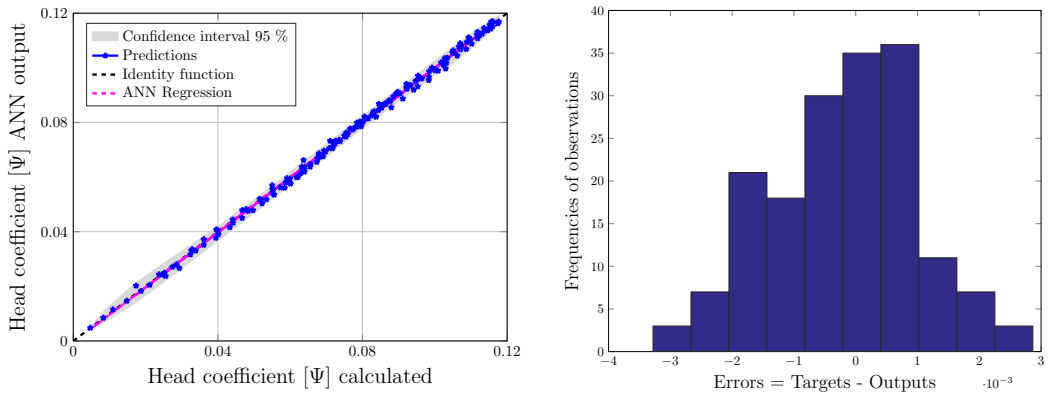

(a) Linear regression. (b) Absolute error distribution.

Figure 6. Validation of the MLP with 2 hidden layers.

The analysis of the parameters for the NNFIR was the same as the MLP but with one more *Lag space*. As shown in Table 4, the MSE error for 1 hidden layer slightly decreased as more *Lag space* was added. Moreover, it was also observed that at the same time the number of hidden layers increased, the MSE error decreased, characterizing a performance gain. For 2 hidden layers with 2 and 3 *Lag space*, the behavior is the same that as explained above. Thus, the architecture with 2 hidden layers with 3 neurons in the first one and 14 in the second one and with 3 *Lag space* was chosen. Figure 7 shows the NNFIR linear regression for the validation data set and the absolute error distribution.

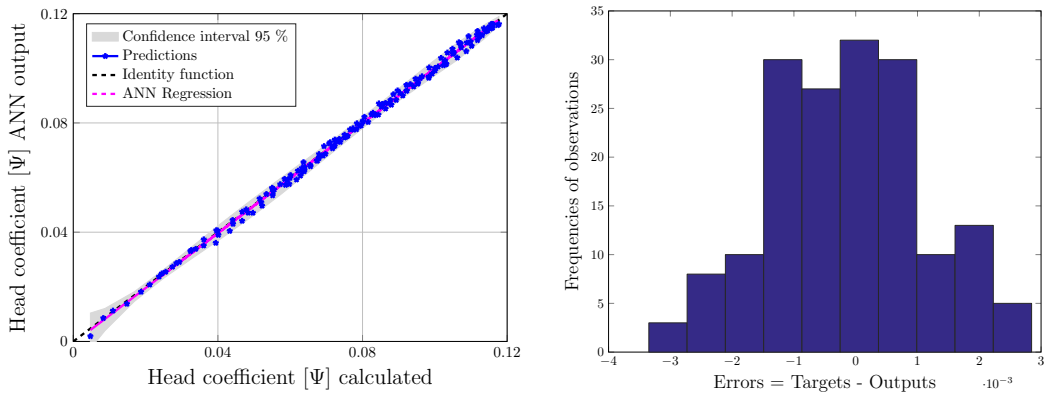

(a) Linear regression. (b) Absolute error distribution.

Figure 7. Validation of the NNFIR with 2 hidden layers for *Lag space* $n = 3$.

In the linear regression shown in figures 6(a) and 7(a), a confidence interval of 95% of the ANN for the validation data is observed. This confidence interval guarantees that any data that enters in the ANN, the result will be within this range. This confidence interval was calculated based on the normal distribution of the absolute error shown in figures 6(b) and 7(b). The result represents a good response from the ANN for the data that has never seen, providing an idea of the generalization capacity of the MLP and the NNFIR.

In order to compare the results with the model proposed by Biazussi (Biazussi, 2014), two groups of data set were taken. Although these groups were not on the training and testing data set, they were measured as well. Those groups are described on Table 5.

Table 5. Data set for comparison between the ANN and mathematical model.

	Rotation Speed [RPM]	Viscosity [cP]	Samples
Test group	2400	203	26
Test group	3000	422	28

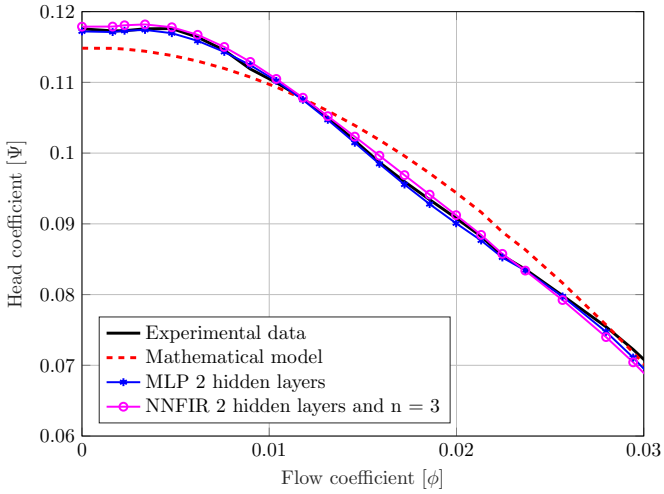

Figure 8. Comparison of ANN and Biazussi model for 2400 RPM and 203 cP.

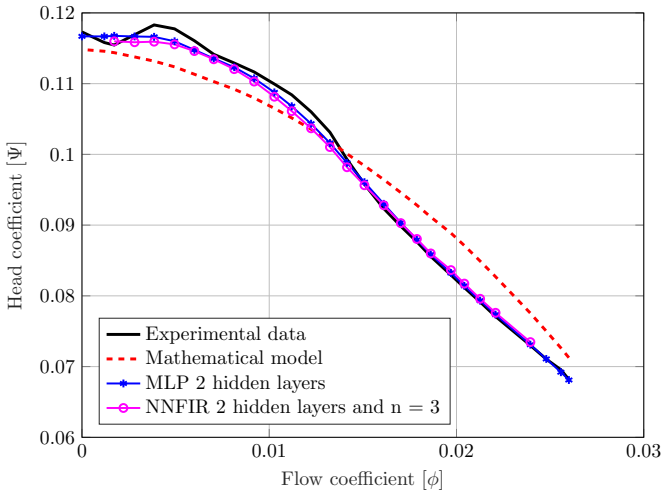

Figure 9. Comparison of ANN and Biazussi model for 3000 RPM and 422 cP.

In Figure 8 and Figure 9, it is possible to see that both ANN structures (MLP and NNFIR) fit well to the validation curve. In this case, the range of training was 1200 to 3500 RPM, and the range of validation was 2400 and 3000 RPM. If the ANN is tested between the range of training, the approximation will be better than the mathematical model. If it is tested outside of this range, the ANN could extrapolate the values.

Besides, the model proposed by Biazussi (Biazussi, 2014) is a good model that describes the ESP performances in different conditions. It can be used to calculate, extrapolate and describe systems. In the range where the ANN is trained, the network will have more accuracy than the analytical model.

5. CONCLUSIONS

An Artificial Neural Network was proposed to describe the ESP performance working with glycerin. To model the ANN, two structures were compared to study the difference in relation to the *Lag space* in the inputs. From the obtained results for the studied case, based on computational cost and possible measurement uncertainties, it is not possible to state that one structure is better than the other. For the NNFIR structure, the computational cost of training is greater than for the MLP, this computational effort does not translate into a representative gain in the obtained results.

Although the computational effort in the training phase of the NNFIR structure with 3 *Lag space* does not have a significant difference in the response with respect to the MLP as shown in figures 8 and 9, the NNFIR structure would have an advantage in a control system, since that the *Lag space* at the inputs would aid in predictive control.

When the ANN is trained and tested in the same range of data, the ANN performance is better than the mathematical model developed by Biazussi (Equation 6), but when the validation data is outside of the training range, the mathematical model is better than the ANN. Thus, the result is difficult to apply to any other type of problem since problems depend on the train range data.

6. ACKNOWLEDGEMENTS

The authors thank Queiroz Galvão E&P, ANP *"Compromisso de Investimentos com Pesquisa e Desenvolvimento"*, PRH/ANP and FAEPEX-UNICAMP (processo 519.292-3227/16) for providing financial support for this work. Acknowledgments are also extended to CEPETRO/UNICAMP and ALFA group *(Artificial Lift & Flow Assurance Research Group)*.

7. REFERENCES

Biazussi, J.L., 2014. *Modelo de Deslizamento para Escoamento Gás-Líquido em Bomba Centrífuga Submersa Operando com Líquido de Baixa Viscosidade*. Ph.D. thesis, Universidade Estadual de Campinas (UNICAMP).

Cruz, P.P., 2010. *Ingeligencia Artificial con Aplicaciones a la Ingeniería*. Alfaomega.

Hagan, M.T. and Menhaj, M.B., 1994. "Training feedforward networks with the marquardt algorithm". *IEEE Transactions on Neural Network*, Vol. 5, No. 6, pp. 989 – 993.

Haykin, S., 2005. *Neural Networks: A comprehensive foundation*. Pearson Prentice Hall.

Haykin, S., 2008. *Neural Networks and Learning Machines*. Pearson Prentice Hall, 3rd edition.

Hornik, K., 1989. "Multilayer feedforward networks are universal approximators". *Neural Networks*, Vol. 2, pp. 359–366.

Hydraulic Institute, 2010. *Effects of Liquid Viscosity on Rotor Dynamic Pump Performance*, ANSIHI 9.6.7-2010.

Monte Verde, W., 2016. *Modelagem do Desempenho de Bombas de BCS Operando com Mistura Gás-Óleo Viscoso*. Ph.D. thesis, Universidade Estadual de Campinas (UNICAMP).

Nørgaard, M., Ravn, O., Poulsen and Hansen, L., 2001. *Neural Networks for Modelling and Control of Dynamics Systems*. Springer.

Paternost, G.M., 2013. *Estudo Experimental Sobre Bomba Centrífuga Operando com Fluido Viscoso e Escoamento Bifásico Gás-Líquido*. Master's thesis, Universidade Estadual de Campinas (UNICAMP).

Priddy, K.L. and Keller, P.E., 1985. *Artificial Neural Networks*. Dover Publications, INC.

Sirilo, T., 2013. *Estudo Numérico da Influência da Viscosidade no Desempenho de uma Bomba Centrífuga Submersa*. Master's thesis, Universidade Tecnológica Federal do Paraná.

Solano, E.A., 2009. *Viscous effects on the performance of electro submersible pumps (ESP's)*. Master's thesis, University of Tulsa.

Stepanoff, A.J., 1957. *Centrifugal and Axial Flow Pumps: Theory, Design and Application*. Krieger Publishing Company.

Takács, G., 2009. *Electrical Submersible Pumps Manual*. Gulf Professional Publishing.

Zambrano, W.C.A., 2013. *Controle Ativo de Vibrações usando Redes Neurais Artificias*. Master's thesis, Universidade Estadual de Campinas (UNICAMP).

8. RESPONSIBILITY NOTICE

The author(s) is (are) the only responsible for the printed material included in this paper.